

Supplement of Atmos. Chem. Phys., 21, 2895–2916, 2021  
<https://doi.org/10.5194/acp-21-2895-2021-supplement>  
© Author(s) 2021. This work is distributed under  
the Creative Commons Attribution 4.0 License.



*Supplement of*

## **Atmospheric VOC measurements at a High Arctic site: characteristics and source apportionment**

**Jakob B. Pernov et al.**

*Correspondence to:* Jakob B. Pernov (jbp@envs.au.dk) and Rossana Bossi (rbo@envs.au.dk)

The copyright of individual parts of the supplement might differ from the CC BY 4.0 License.

## 1. Mixing Ratio and Uncertainty Calculation

Mixing ratios were calculated, in the absence of suitable reference materials, according to Equation S1, using the reaction kinetics quantification method.

$$R_{ppb} = \frac{RH^+ \times 10^9 \times U \times 2.8 \times 22400 \times 1013^2 \times T^2 \times Tr_{(H_3^{18}O^+)}}{k \times 9.2^2 \times H_3^{18}O^+ \times 500 \times P^2 \times 6.02 \times 10^{23} \times 273.15^2 \times Tr_{(RH^+)}} \quad (S1)$$

Where  $R_{ppb}$  is the mixing ratio of the analyte ion R,  $RH^+$  is the raw signal of the protonated analyte in cps,  $10^9$  is the conversion to ppb,  $U$  is the voltage of the drift tube in volts, 2.8 is the reduced ion mobility (which has been experimentally determined) in  $cm^2/Vs$ , 22400 is the molar volume in moles per  $cm^3$ , 1013 is standard pressure in mbar,  $T$  is the temperature of the drift tube in K,  $Tr_{(H_3^{18}O^+)}$  is the transmission of the primary ion isotope ( $H_3^{18}O^+$ ),  $k$  is the rate reaction coefficient of the analyte ion with the hydronium ion, 9.2 is the length of the drift tube in cm,  $H_3^{18}O^+$  is the raw signal of the isotope of the primary ion, 500 is the isotopic ratio correction factor,  $P$  is the pressure of the drift tube in mbar,  $6.02 \times 10^{23}$  is Avogadro's number in molecules per mole, 273.15 is standard temperature, and  $Tr_{(RH^+)}$  is the transmission of the protonated analyte ion. The isotope of the primary ion is used to avoid detector saturation. It must be noted that due to the backreaction of formaldehyde with water vapor in the drift tube, mixing ratios of formaldehyde are likely a lower limit (Holzinger et al., 2019; Hansel et al., 1997). However, due to the low absolute humidity levels in the Arctic, this reaction is negligible, furthermore, no correlation was observed between humidity (absolute or relative) and formaldehyde.

In the absence of suitable reference materials, an uncertainty budget was created based on the formula for kinetic calibration Eq. (S1). There are terms in Eq. (S1) that are assumed negligible including drift temperature, drift pressure, and ion transmission. These components are deemed negligible because they either are measured with high accuracy (temperature and pressure) or are lacking empirical error analysis (ion transmission). The greatest sources of uncertainty in this equation are the rate reaction coefficient and the counts of the primary ion and the analyte ion. According to Cappellin et al. (2010), the relative uncertainty of their rate reaction coefficients is stated at 15 %. The uncertainty from the raw ion cps was determined from the counting statistics by assuming a Poisson distribution (Hayward et al., 2002). The standard uncertainty for the ion counts is, therefore, the square root of the cps multiplied by the signal integration time (5 s). The analyte signal was blank corrected before uncertainty analysis. The expanded uncertainty is then calculated according to Eq. (S2), using a coverage factor of two.

$$U = 2 \times VMR \times \sqrt{0.15^2 + \left(\frac{\sqrt{I_P}}{I_P}\right)^2 + \left(\frac{\sqrt{I_{S-b}}}{I_{S-b}}\right)^2} \quad (S2)$$

Where  $U$  is the expanded uncertainty,  $VMR$  is the volume-mixing ratio,  $I_P$  is the raw counts of the primary ion,  $I_{S-b}$  is the blank corrected counts of the analyte ion.

## 2. Quality Control Procedure

Data were quality controlled by analysis of PNSD, ozone, wind direction and speed, and internal activity logs. Local pollution at Villum can arise from activity around the measurement site (e.g., passenger vehicles, all-terrain vehicles, snowmobiles, and heavy machinery) as well as from activities from Station Nord (e.g., waste incineration, vehicular activity, and aircraft landing, idling, and take off). Internal activity logs of visits to the measurement building were used to highlight periods when human activity could affect the measurements, periods where VOC levels were elevated over background levels for the duration of the visit to the station were removed. Measurements of PNSD and ozone were analyzed, in tandem, for sharp and sudden increases in the ultrafine mode ( $< 100$  nm) aerosol particles and concurrent sharp and sudden decreases in ozone, increases in ultrafine mode particles are indications of vehicular emissions while decreases in ozone results from its titration with nitrogen oxides. These periods were further inspected for wind direction and speed, with winds coming from due north at low speeds indicative of local pollution from Station Nord. All periods where local pollution was suspected of influencing the measurements were visually inspected by a panel of three persons, a consensus was required before data were removed. Data were also quality controlled for abnormal levels of instrumental parameters (i.e., E/N ratio, drift tube temperature, pressure, and voltage), periods with large deviations from nominal values were removed. Certain compounds (DMS, formic acid, and acetic acid) exhibited a slow return to nominal values after a blank than before, this issue was especially evident in the summer, these periods were removed. All quality control was performed on VOCs at a 5 s time resolution, data was removed before averaging to 30-minute means.

55

**Table S1.** Statistics for meteorological parameters (mean  $\pm$  s.d.) for all seasons, spring (April 4 – June 8), summer (June 9 – August 6), and autumn (August 7 – October 25). During the campaign, there were several large gaps in the data, most noticeably one in July and one in August, as seen in Fig. 1. The seasons are therefore divided based on the continuous collection of data uninterrupted by large missing gaps. The seasons roughly correspond to the conventional definition of seasons.

	All Seasons	Spring	Summer	Autumn
Wind Direction, $^{\circ}$	207.5 $\pm$ 89.0	202.4 $\pm$ 91.8	189.3 $\pm$ 2.6	223.8 $\pm$ 81.2
Wind Speed, m s $^{-1}$	3.3 $\pm$ 2.6	3.1 $\pm$ 2.4	3.5 $\pm$ 2.4	3.4 $\pm$ 2.7
Temperature, $^{\circ}$ C	-6.5 $\pm$ 9.6	-13.8 $\pm$ 9.0	2.2 $\pm$ 4.1	-7.0 $\pm$ 7.9
RH, %	77.4 $\pm$ 12.6	74.6 $\pm$ 10.6	78.0 $\pm$ 15.6	79.1 $\pm$ 11.4
Radiation, W m $^{-2}$	174.9 $\pm$ 163.9	222.3 $\pm$ 146.3	295.9 $\pm$ 4.2	57.0 $\pm$ 97.4
Pressure, hPa	1010.6 $\pm$ 9.0	1014.8 $\pm$ 8.6	1007.5 $\pm$ 6.5	1009.6 $\pm$ 9.5
Snow Depth, m	0.9 $\pm$ 0.6	1.4 $\pm$ 0.1	1.1 $\pm$ 0.4	0.3 $\pm$ 0.4

60

**Table S2.** Total hours of operation of the PTR-ToF-MS for each month of the campaign and for each compound. Periods removed through the QC procedure are not included.

	April	May	June	July	August	September	October
Formaldehyde	374	601	288	661	417	443	403
Acetonitrile	229	601	288	661	417	443	403
Formic Acid	349	601	288	641	417	443	403
Acetone	376	601	288	661	417	443	403
Acetic Acid	375	577	288	661	417	411	359
DMS	300	577	169	391	357	443	377
MEK	376	601	288	661	417	443	403
C <sub>3</sub> H <sub>6</sub> O <sub>2</sub>	327	601	288	661	417	443	403
Benzene	376	601	288	661	417	443	403
C <sub>5</sub> H <sub>8</sub> O	376	601	288	661	417	443	403

**Table S3:** Pearson correlation coefficients <sup>a</sup> for chemical species, temperature and sun radiation measured during April at Villum.

April 2018	Formaldehyde	Acetonitrile	Formic Acid	Acetone	Acetic Acid	DMS	MEK	Benzene	C <sub>3</sub> H <sub>6</sub> O <sub>2</sub>	Temperature	Radiation	Ozone
Formaldehyde	1.00											
Acetonitrile	0.70	1.00										
Formic Acid	0.76	0.45	1.00									
Acetone	0.40	0.30	<i>-0.03</i>	1.00								
Acetic Acid	-0.63	-0.74	-0.45	-0.32	1.00							
DMS	-0.47	-0.67	-0.16	-0.55	0.84	1.00						
MEK	0.52	0.20	0.76	0.03	-0.27	-0.07	1.00					
Benzene	0.27	0.04	0.70	-0.43	<i>-0.07</i>	0.24	0.84	1.00				
C <sub>3</sub> H <sub>6</sub> O <sub>2</sub>	-0.52	-0.66	-0.25	-0.41	0.90	0.94	-0.15	0.11	1.00			
Temperature	-0.47	-0.34	-0.75	0.16	0.54	0.23	-0.74	-0.77	0.46	1.00		
Radiation	-0.26	-0.26	-0.38	0.28	0.20	<i>0.06</i>	-0.25	-0.34	0.21	0.34	1.00	
Ozone	-0.52	-0.48	-0.21	-0.83	0.56	0.64	-0.26	0.15	0.59	0.17	-0.12	1.00

<sup>a</sup> All correlations, apart from the numbers typed in italics, have linear regression p-values below 0.01.

**Table S4:** Pearson correlation coefficients <sup>a</sup> for chemical species, temperature and sun radiation measured during July at Villum.

July 2018	Formaldehyde	Acetonitrile	Formic Acid	Acetone	Acetic Acid	DMS	MEK	Benzene	C <sub>3</sub> H <sub>6</sub> O <sub>2</sub>	Temperature	Radiation	Ozone
Formaldehyde	1.00											
Acetonitrile	0.71	1.00										
Formic Acid	0.88	0.57	1.00									
Acetone	0.86	0.89	0.82	1.00								
Acetic Acid	0.85	0.58	0.95	0.85	1.00							
DMS	0.36	<i>0.01</i>	0.50	0.23	0.42	1.00						
MEK	0.85	0.55	0.93	0.81	0.97	0.41	1.00					
Benzene	0.57	0.50	0.50	0.61	0.59	0.26	0.60	1.00				
C <sub>3</sub> H <sub>6</sub> O <sub>2</sub>	0.83	0.57	0.95	0.82	0.97	0.39	0.95	0.50	1.00			
Temperature	0.65	0.85	0.54	0.82	0.58	<i>0.08</i>	0.54	0.45	0.54	1.00		
Radiation	0.49	0.23	0.59	<i>0.40</i>	0.51	0.26	0.53	0.15	0.56	0.31	1.00	
Ozone	0.54	0.82	0.39	<i>0.69</i>	0.39	0.18	0.33	0.43	0.33	0.76	0.07	1.00

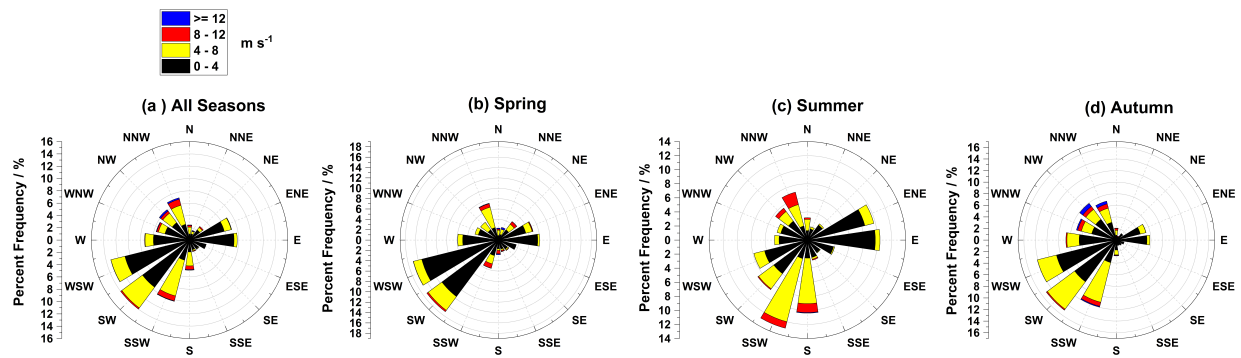
75 <sup>a</sup> All correlations, apart from the numbers typed in italics, have linear regression p-values below 0.01.

**Table S5:** Pearson correlation coefficients <sup>a</sup> for chemical species, temperature and sun radiation measured during September at Villum.

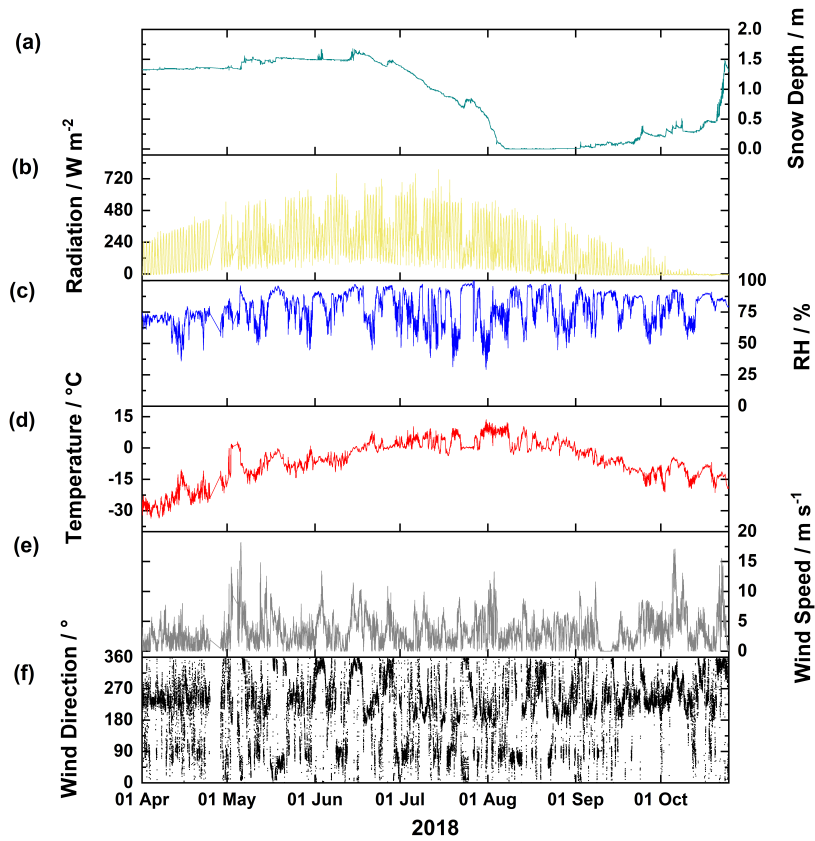
80

September 2018	Formaldehyde	Acetonitrile	Formic Acid	Acetone	Acetic Acid	DMS	MEK	Benzene	C <sub>3</sub> H <sub>6</sub> O <sub>2</sub>	Temperature	Radiation	Ozone
Formaldehyde	1.00											
Acetonitrile	0.61	1.00										
Formic Acid	0.76	0.45	1.00									
Acetone	0.72	0.96	0.57	1.00								
Acetic Acid	<i>0.06</i>	0.29	<i>0.07</i>	0.28	1.00							
DMS	-0.29	-0.76	-0.18	-0.68	-0.10	1.00						
MEK	0.82	0.71	0.64	0.79	0.43	-0.35	1.00					
Benzene	0.50	0.15	0.42	0.19	0.21	0.25	0.61	1.00				
C <sub>3</sub> H <sub>6</sub> O <sub>2</sub>	0.76	0.35	0.62	0.43	0.12	<i>-0.03</i>	0.69	0.64	1.00			
Temperature	-0.81	-0.35	-0.77	-0.53	0.26	0.10	-0.58	-0.40	-0.68	1.00		
Radiation	<i>-0.07</i>	<i>-0.04</i>	-0.09	-0.06	0.29	-0.07	<i>0.01</i>	-0.11	-0.10	0.33	1.00	
Ozone	0.74	0.70	0.63	0.79	0.14	-0.26	0.72	0.31	0.56	-0.64	-0.23	1.00

<sup>a</sup> All correlations, apart from the numbers typed in italics, have linear regression p-values below 0.01.



85 **Fig. S1.** Wind Rose for mean wind speed at 5 min time resolution for (a) all seasons, (b) spring, (c) summer, and (d) autumn. The y-axis represents the percent frequency of wind direction in percent and the colors indicate mean wind speed in  $\text{m s}^{-1}$ . The seasons follow the selection outlined in Table S1.



90

**Fig. S2.** Time series meteorological parameters **(a)** snow depth, **(b)** radiation, **(c)** relative humidity (RH), **(d)** temperature, **(e)** wind speed, and **(f)** wind direction during the entire measurement period.

95

## Diurnal Profile for Spring

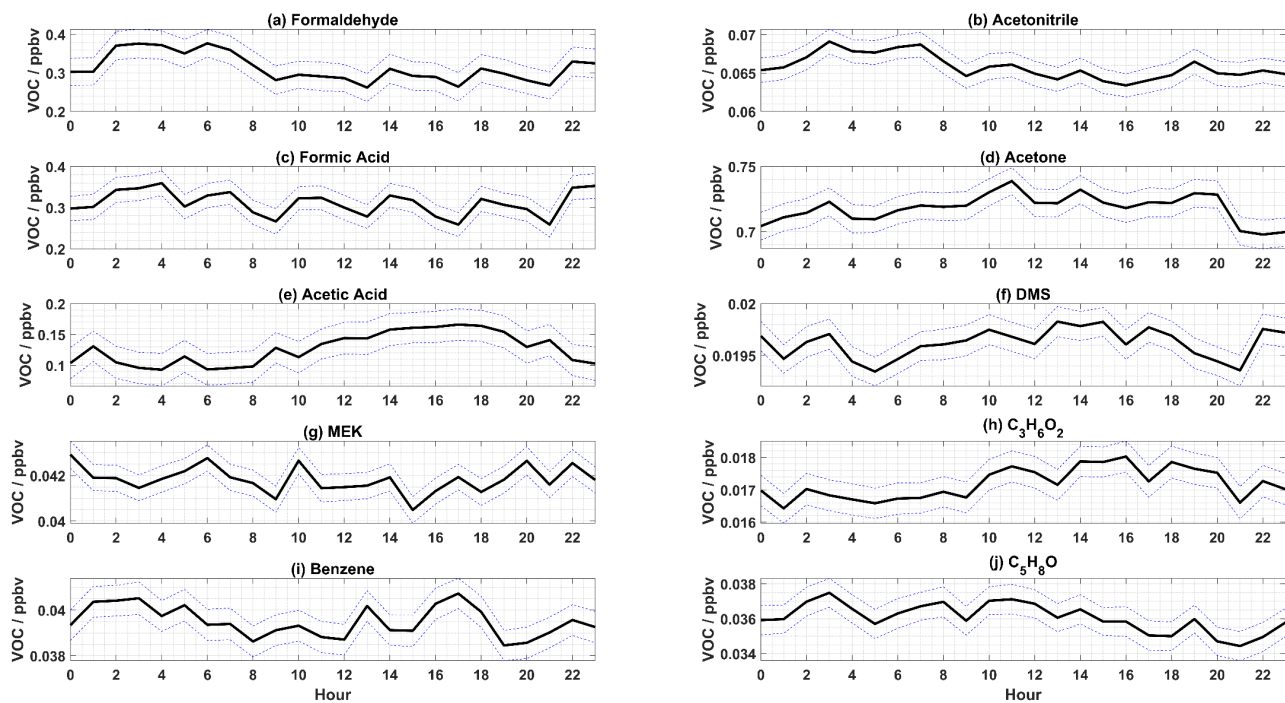


**Fig. S3.** Diurnal profile for the spring (April–May) of **(a)** formaldehyde, **(b)** acetonitrile, **(c)** formic acid, **(d)** acetone, **(e)** acetic acid, **(f)** DMS, **(g)** MEK, **(h)**  $C_3H_6O_2$ , **(i)** benzene, **(j)**  $C_5H_8O$ . Data were averaged to hourly medians. The blue dotted lines represent the 95 % confidence interval.

### Diurnal Profile for Summer

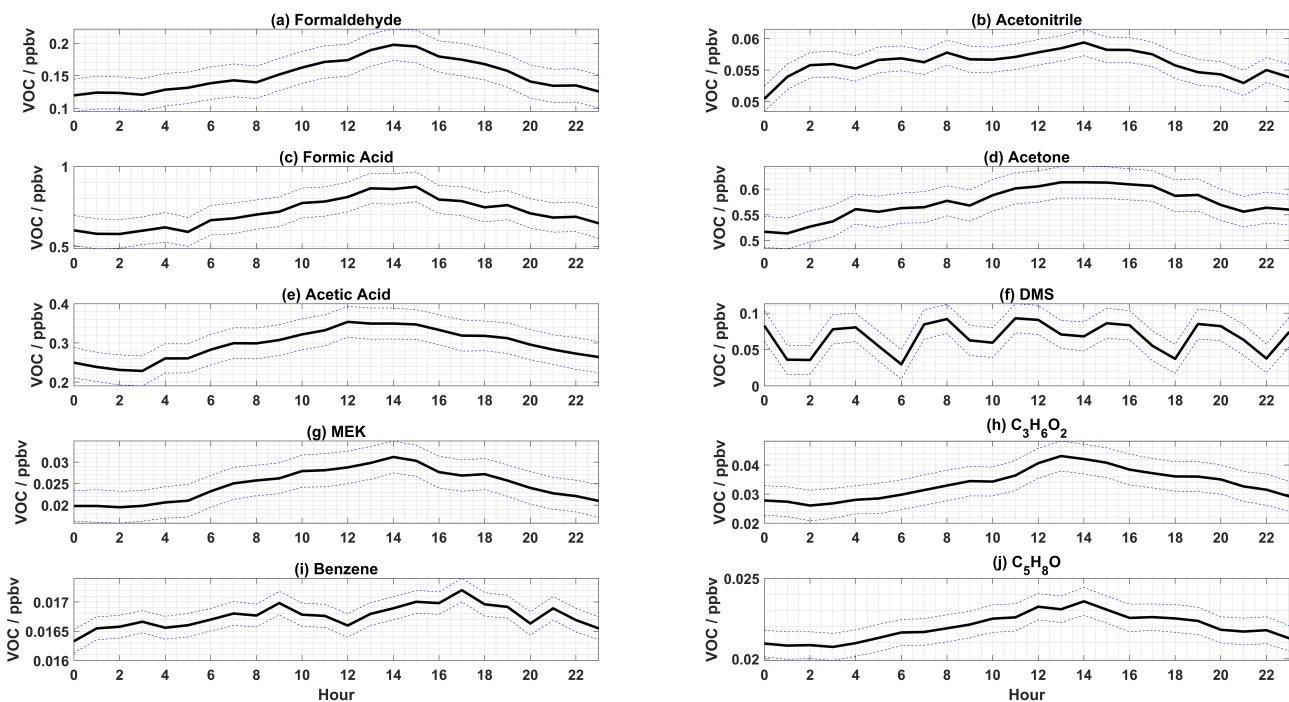


**Fig. S4.** Diurnal profile for the summer (June–August) of **(a)** formaldehyde, **(b)** acetonitrile, **(c)** formic acid, **(d)** acetone, **(e)** acetic acid, **(f)** DMS, **(g)** MEK, **(h)**  $C_3H_6O_2$ , **(i)** benzene, **(j)**  $C_5H_8O$ . Data were averaged to hourly medians. The blue dotted lines represent the 95 % confidence interval.

### Diurnal Profile for Autumn

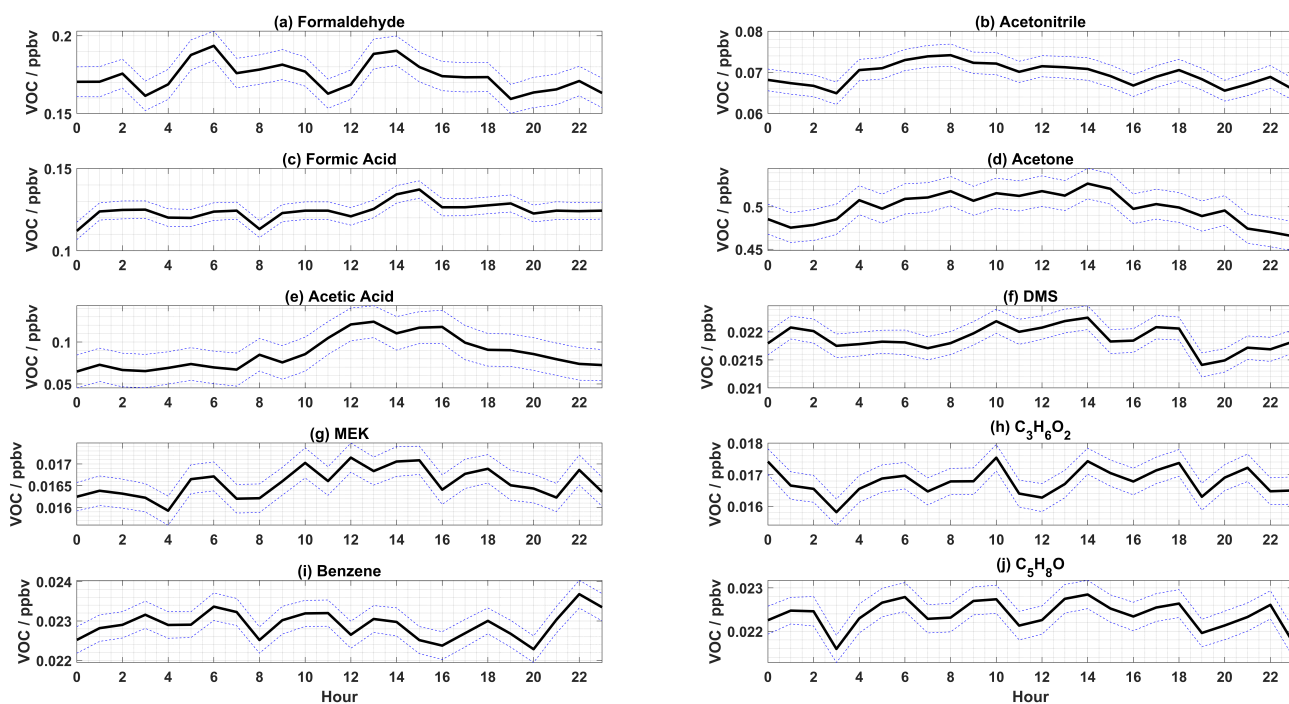
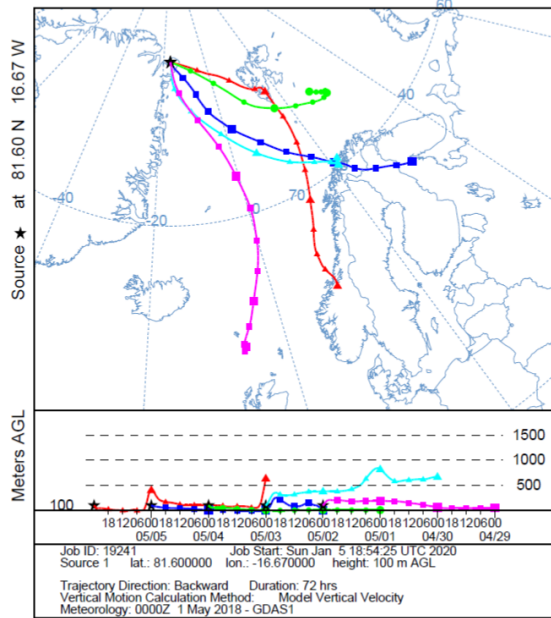
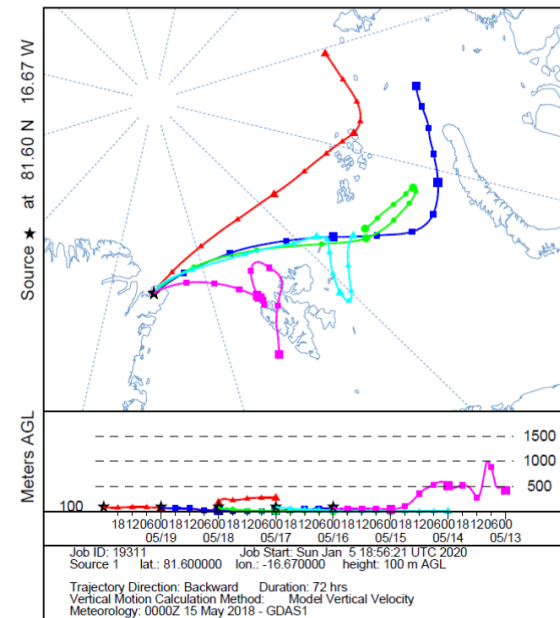


**Fig. S5.** Diurnal profile for the autumn (September–October) of **(a)** formaldehyde, **(b)** acetonitrile, **(c)** formic acid, **(d)** acetone, **(e)** acetic acid, **(f)** DMS, **(g)** MEK, **(h)** C<sub>3</sub>H<sub>6</sub>O<sub>2</sub>, **(i)** benzene, **(j)** C<sub>5</sub>H<sub>8</sub>O. Data were averaged to hourly medians. The blue dotted lines represent the 95 % confidence interval.

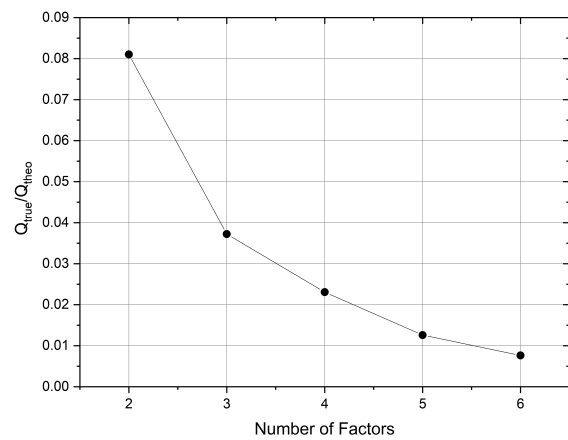
(a) NOAA HYSPLIT MODEL  
Backward trajectories ending at 0000 UTC 06 May 18  
GDAS Meteorological Data



(b) NOAA HYSPLIT MODEL  
Backward trajectories ending at 0000 UTC 20 May 18  
GDAS Meteorological Data



120 **Fig. S6.** HYSPLIT back trajectory analysis for **(a)** May 2<sup>nd</sup>– 6<sup>th</sup> **(b)** May 16<sup>th</sup>–20<sup>th</sup> arriving at 100 m above ground level extending 72 hours backward in time. The colored trajectories represent a new trajectory started every 24 hours after the last day of each period until the first day, in descending order the trajectories are red (last day), blue (fourth day), green (third day), light blue (second day), and purple (first day).



125

**Fig. S7.** The ratio of  $Q_{\text{true}}$  to  $Q_{\text{theo}}$  versus the number of factors for the PMF analysis.

130

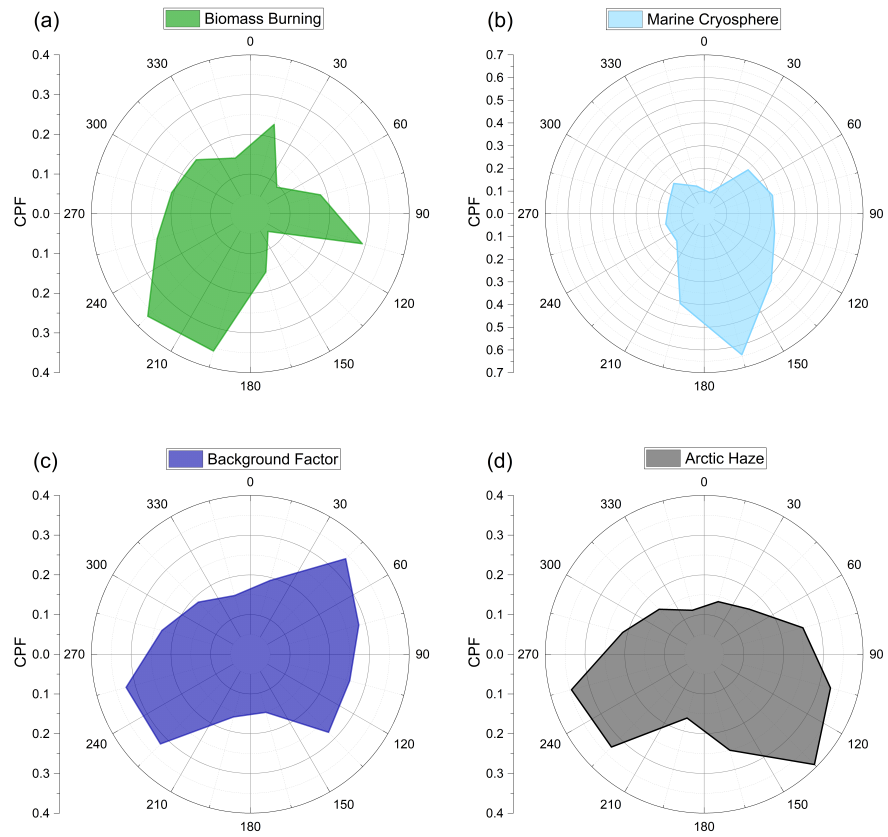


**Fig. S8.** Conditional probability function roses for **(a)** Biomass Burning Factor, **(b)** Marine Cryosphere Factor, **(c)** Background Factor, and **(d)** Arctic Haze Factor.

## References

- 140 Cappellin, L., Probst, M., Limtrakul, J., Biasioli, F., Schuhfried, E., Soukoulis, C., Märk, T. D., and Gasperi, F.: Proton transfer reaction rate coefficients between  $\text{H}_3\text{O}^+$  and some sulphur compounds, *International Journal of Mass Spectrometry*, 295, 43-48, 10.1016/j.ijms.2010.06.023, 2010.
- Hansel, A., Singer, W., Wisthaler, A., Schwarzmann, M., and Lindinger, W.: Energy dependencies of the proton transfer reactions  $\text{H}_3\text{O}^+ + \text{CH}_2\text{O} \rightleftharpoons \text{CH}_2\text{OH}^+ + \text{H}_2\text{O}$ , *International Journal of Mass Spectrometry and Ion Processes*, 167-168, 697-703, [https://doi.org/10.1016/S0168-1176\(97\)00128-6](https://doi.org/10.1016/S0168-1176(97)00128-6), 1997.
- 145 Hayward, S., Hewitt, C. N., Sartin, J. H., and Owen, S. M.: Performance characteristics and applications of a proton transfer reaction-mass spectrometer for measuring volatile organic compounds in ambient air, *Environmental Science & Technology*, 36, 1554-1560, 10.1021/es0102181, 2002.
- 150 Holzinger, R., Acton, W. J. F., Bloss, W. J., Breitenlechner, M., Crilley, L. R., Dusanter, S., Gonin, M., Gros, V., Keutsch, F. N., Kiendler-Scharr, A., Kramer, L. J., Krechmer, J. E., Languille, B., Locoge, N., Lopez-Hilfiker, F., Materić, D., Moreno, S., Nemitz, E., Quéléver, L. L. J., Sarda Esteve, R., Sauvage, S., Schallhart, S., Sommariva, R., Tillmann, R., Wedel, S., Worton, D. R., Xu, K., and Zaytsev, A.: Validity and limitations of simple reaction kinetics to calculate concentrations of organic compounds from ion counts in PTR-MS, *Atmospheric Measurement Techniques*, 12, 6193-6208, 10.5194/amt-12-6193-2019, 2019.